# The chemokine CXCL16 can rescue the defects in insulin signaling and sensitivity caused by palmitate in C2C12 myotubes

**Stavroula Bitsi***

Comparative Biomedical Sciences Department, Royal Veterinary College, London NW1 0TU, United Kingdom.

*corresponding author: sbitsi@rvc.ac.uk

Present address: Section of Cell Biology and Functional Genomics, Imperial College London, London W12 0NN, United Kingdom.

# ABSTRACT

In obesity, macrophages infiltrate peripheral tissues and secrete pro-inflammatory cytokines that impact local insulin sensitivity. Lipopolysaccharide (LPS) and the saturated fatty acid (FA) palmitate polarise macrophages towards a pro-inflammatory phenotype *in vitro* and indirectly cause insulin resistance (IR) in myotubes. In contrast, unsaturated FAs confer an anti-inflammatory phenotype and counteract the actions of palmitate. To explore paracrine mechanisms of interest, J774 macrophages were exposed to palmitate ± palmitoleate or control medium and the conditioned media generated were screened using a cytokine array. Of the 62 cytokines examined, 8 were significantly differentially expressed following FA treatments. Notably, CXCL16 secretion was downregulated by palmitate. In follow-up experiments using ELISAs, this downregulation was confirmed and reversed by simultaneous addition of palmitoleate or oleate, while LPS also diminished CXCL16 secretion. To dissect potential effects of CXCL16, C2C12 myotubes were treated with palmitate to induce IR, recombinant soluble CXCL16 (sCXCL16), combined treatment, or control medium. Palmitate caused the expected reduction of insulin-stimulated Akt activation and glycogen synthesis, whereas simultaneous treatment with sCXCL16 attenuated these effects. These data indicate a putative role for CXCL16 in preservation of Akt activation and insulin signaling in the context of chronic low-grade inflammation in skeletal muscle.



***Keywords:*** obesity, insulin resistance, CXCL16, macrophage, muscle


***Abbreviations:*** Akt: v-akt murine thymoma viral oncogene homolog, AT: adipose tissue, CM: conditioned medium, ELISA: enzyme-linked immunosorbent assay, ERK1/2: extracellular signal-regulated kinases 1/2, FA: fatty acid, IL: interleukin, IR: insulin resistance, LPS: lipopolysaccharide, GSK: glycogen synthase kinase, MCP: monocyte chemoattractant protein, MIP: Macrophage inflammatory protein, NK: natural killer, NKT: natural killer T, PA: palmitate, PF-4: platelet factor 4, PO: palmitoleate, sCXCL16: soluble C-X-C Motif Chemokine Ligand 16, SFA: saturated fatty acid, sTNFRI: Soluble tumor necrosis factor receptor I, T2D: type 2 diabetes, TNF-α: tumor necrosis factor-α, UFA: unsaturated fatty acid

# 1. INTRODUCTION

Obesity, defined by the World Health Organization as 'abnormal or excessive fat accumulation that may impair health' [1], constitutes one of the major risk factors for type 2 diabetes (T2D). T2D prevalence has increased in recent decades, with the number of diagnosed adults rising from 108 million in 1980 to 422 million in 2014 [2]. A blunted response to insulin leading to impaired glucose uptake and utilization in target tissues termed as insulin resistance (IR) is a key characteristic of T2D [3]. It can arise in obesity [4] and is a known risk factor for T2D development [5]. IR can precede the manifestation of overt hyperglycemia for over a decade [6] and, therefore, identifying and treating IR in a timely fashion can be important for avoiding progression to T2D.

A state of chronic low-grade inflammation has been noted in obesity [7, 8] and linked to IR and T2D development. The first observation at the tissue level was an increase in tumor necrosis factor (TNF)-α secretion by adipose tissue (AT) from obese rodents that led to IR [9, 10]. This increased secretion was later attributed mainly to local accumulation of macrophages forming 'crown-like' structures surrounding dying adipocytes [11-13]. It is thought that an imbalance of M1 'classically activated' macrophages that secrete proinflammatory cytokines and M2 'alternatively activated' macrophages that are anti-inflammatory and insulin-sensitizing might arise and cause complications [14]. There are discrepancies between studies concerning the action of certain cytokines, and studies targeting immune components have so far yielded mixed results. For instance, monocyte chemoattractant protein (MCP)-1, one of the most studied chemokines in inflammation-associated IR, is upregulated in diet-induced obesity and studies using *in vitro* and knock-out [15, 16] or transgenic overexpressing [17] *in vivo* MCP-1 deficiency only partially restores insulin sensitivity in AT [18] and skeletal muscle [15] in mice-fed a HFD. Cytokines are pleiotropic molecules and multiple cytokines can shape the pro-inflammatory phenotype seen in obesity; thus, the complexity and redundancy of immune system activation in obesity call for further investigation. Recently, a 'designer cytokine', IC7Fc, an engineered fusion of interleukin (IL)-6 and ciliary

58 neurotrophic factor, ameliorated glucose tolerance and decreased weight gain in obese mice, opening up
59 a promising chapter for the use of novel biological agents in the treatment of T2D [19].

60 Initial studies in the field focused on inflammation in expanding AT; however, infiltration of macrophages
61 has also been documented in skeletal muscle in obesity [15, 20-22], which might have implications for
62 whole-body insulin sensitivity since muscle is the major site of postprandial glucose uptake and utilization
63 [23]. To dissect the interplay between macrophages and myotubes, experiments employing *in vitro*
64 models have used macrophage conditioned medium (CM) to treat myotubes in culture in an attempt to
65 isolate the interaction between these two cell types. Elevated free fatty acids (FAs) [24, 25] and
66 lipopolysaccharide (LPS) [26-29] have been documented in obesity and T2D and have been associated
67 with the pathogenesis of IR. *In vitro*, LPS and the saturated FA (SFA) palmitate polarize macrophages
68 towards a pro-inflammatory 'M1' phenotype, whereas the unsaturated FAs (UFAs) palmitoleate and
69 oleate confer an anti-inflammatory 'M2' phenotype [30-33]. Several studies have indicated differential
70 effects of palmitate and UFAs as well as LPS on macrophage gene expression and secretome [30-32, 34-
71 37]. CM generated by palmitate-treated macrophages (PA CM) has been shown to induce IR in myotubes,
72 while CM from UFA-treated macrophages is insulin-sensitizing [31, 38, 39]. The components of PA CM
73 that might be of relevance are still being established, but a study by Talbot et al. put forward TNF-α, a
74 known major inflammatory mediator of IR in myocytes [40], as a strong candidate [31]. The mechanisms
75 underlying the indirect effects of UFAs are less clear. Talbot et al. demonstrated that CM generated by
76 macrophages treated with palmitate plus palmitoleate (PA+PO CM) did not have detrimental actions on
77 insulin sensitivity of myotubes in contrast to PA CM [31], suggesting that addition of palmitoleate alters
78 the macrophage secretome in a favorable way. The mediators that differ between PA CM and PA+PO CM
79 involved in these differential indirect effects on myotubes have not been clarified. Thus, following on
80 from the study by Talbot and colleagues, the same CM model established in the lab was employed to
81 examine the secretome of J774 macrophages and establish how FAs and LPS may differentially modify it,

as well as identify mediators not previously studied. The use of a cytokine array allowed for screening of 62 candidate cytokines/chemokines potentially involved in pro-/anti-inflammatory actions, chemotaxis, adhesion and regulation of insulin sensitivity.

## 2. RESULTS

### *2.1. Screening of J774 CM using a cytokine array reveals differential secretion upon treatment with palmitate*

In order to screen J774 CM for cytokines and chemokines of interest, a cytokine array was selected comprising cytokines that have been implicated in both pro- and anti-inflammatory functions as well as cytokines and chemokines that have not been studied before in the context of inflammation-associated IR. 500 µM palmitate was used, as this concentration has been shown to polarize macrophages towards a pro-inflammatory phenotype [38, 41]. Combined treatment with palmitoleate was used as palmitoleate has been shown to counteract the effects of palmitate [31]. The results for 62 cytokines were analyzed. Figure 1 focuses on those whose levels were significantly affected by FA treatment.

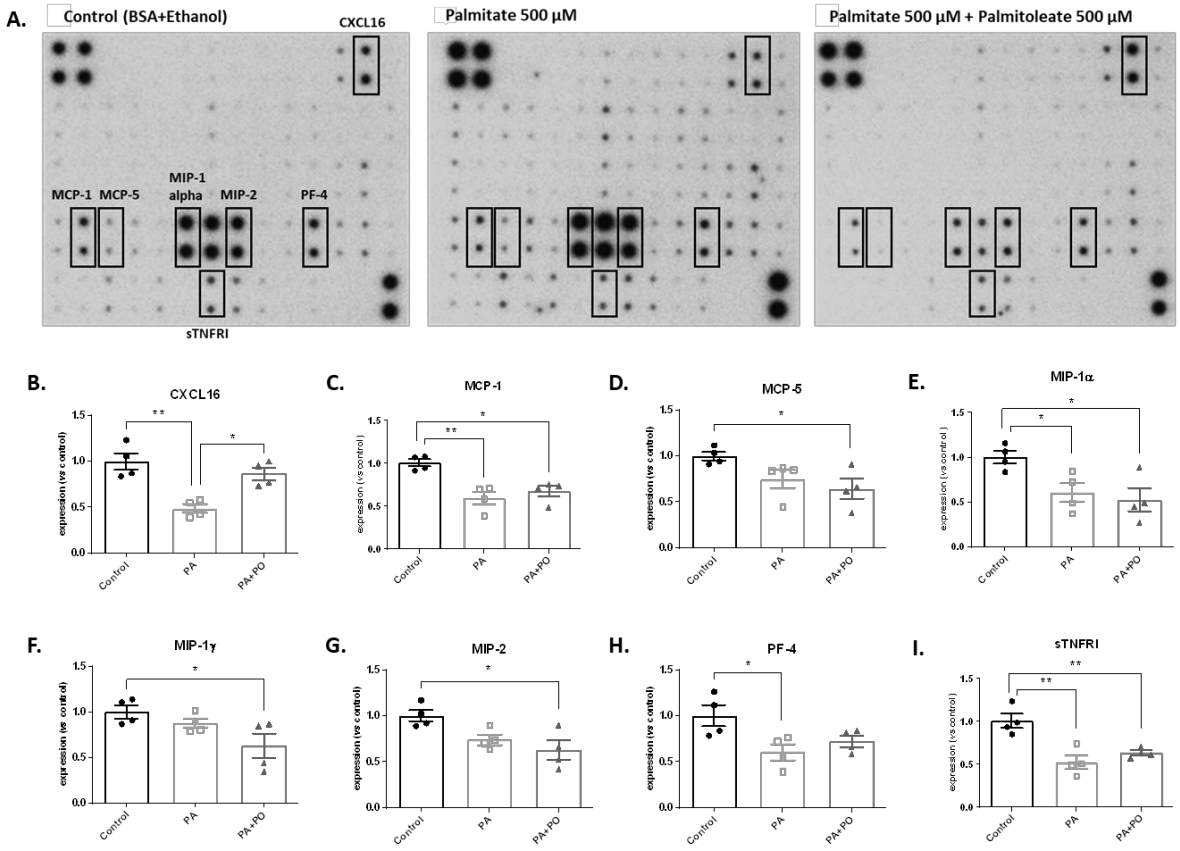


**Figure 1. Cytokines and chemokines that are differentially regulated with FA treatments compared to control. A.** Representative blots from cytokine array membranes incubated with CM from J774 pre-treated with control, palmitate 500 µM and palmitate 500 µM + palmitoleate 500 µM. The location of selected chemokines and cytokines is marked. **B.** CXCL16. **C.** MCP-1. **D.** MCP-5. **E.** MIP-1α. F. MIP-1γ. **G.** MIP-2. **H.** PF-4. **I.** sTNFRI. Fold expression of cytokines and chemokines relative to control (BSA+Ethanol). Data are presented as mean ± SEM analyzed by one-way ANOVA followed by Tukey's *post hoc* analysis (n=4). *p<0.05, **p<0.01 vs control.

8 cytokines were affected by treatment with PA and PA+PO CM. Specifically, C-X-C Motif Chemokine Ligand 16 (CXCL16) was downregulated in PA CM by 52% compared to control CM (p<0.01), while secretion in PA+PO CM was comparable to control CM. Platelet factor 4 (PF-4) secretion in PA CM was decreased by 39% compared to control (p<0.05), while MIP-1α secretion had a similar decrease of 40% in

PA CM compared to control ($p<0.05$). Soluble tumor necrosis factor receptor I (sTNFRI) secretion was reduced by 48% in PA CM and 37% in PA+PO CM ($p<0.01$ vs control). Similarly, MCP-1 was reduced in both PA CM (by 41%, $p<0.01$) and PA+PO CM (by 33%, $p<0.05$) compared to control CM. Secretion of MCP-5, MIP-1α, MIP-1γ and MIP-2 were all decreased in PA+PO CM (by 36%, 47%, 38% and 38% *versus* control CM, respectively, $p<0.05$). The results for the remaining cytokines that were analyzed but were not significantly altered by the treatments are presented at Supplementary Figure 2.

### *2.2. Validation of differential expression of chemokines and cytokines of interest using ELISA*

Appropriate controls to account for intra- and inter- assay variability were used when calculating the results. However, antibody arrays can have limitations associated with high-throughput screening assays as well as protein-protein interactions [42-44]. Therefore, it was decided to validate the data for differentially expressed cytokines using specific ELISAs, which also allow for absolute quantification of cytokine concentrations in CM.

500 µM palmitate was used in the experiments for array analysis to mirror previous literature using high concentrations of palmitate, in accordance with reports of elevated palmitate in obese and insulin-resistant individuals. However, to make sure that the results were not compromised by lower cell numbers due to loss of viability (see Supplementary Figure 3), the validation experiments were performed using FAs at 200 µM. In addition to palmitate and the combination of palmitate+palmitoleate, other FA treatments were also tested (palmitoleate alone, oleate, palmitate + oleate, palmitoleate + oleate) as well as LPS. 200 µM palmitate has been reported to alter macrophage gene expression, differentially to LPS, while 200 µM oleate had no effect [37].

Of the 8 differentially secreted cytokines and chemokines, CXCL16, MCP-1, PF-4, MIP-1α, MIP-2, and sTNFRI were validated using ELISA. MCP-5 is a murine chemokine, with no known equivalent for humans [45], so it was not examined further. The results of the ELISAs are presented in Figure 2.

Regulation of CXCL16 secretion was confirmed, as palmitate significantly decreased its secretion by 56% compared to control (mean ± SD: 690.5 ± 255.3 pg/mL vs 1572 ± 447.6 pg/mL, $p<0.01$). Simultaneous incubation of palmitate with oleate or palmitoleate, restored secretion to control levels (1700 ± 211.1 pg/mL and 1562 ± 213.6 pg/mL respectively, $p>0.05$ vs control). Intriguingly, LPS also decreased CXCL16 secretion by 47% compared to control (836.4 ± 201.4 pg/mL, $p<0.05$ vs control). Secretion of sTNFRI followed a pattern similar to that identified by the cytokine array for palmitate incubation, although the reduction, compared to control, did not reach statistical significance (197 ± 24.63 pg/mL in PA CM vs 408.4 ± 25.37 in control CM, $p=0.11$). There was no reduction observed for PA+PO CM (328.8 ± 53.22, $p>0.05$ vs control CM). Nevertheless, significant differences were observed between LPS and PA as well as PO treatments. There was a 65% decrease in PA CM compared to LPS CM (197 ± 24.63 pg/mL vs 557.1 ± 184.4 pg/mL respectively, $p<0.01$) and a 47% decrease in PO CM compared to LPS CM (294.8 ± 56.7 pg/mL vs 557.1 ± 184.4 pg/mL respectively, $p<0.05$).

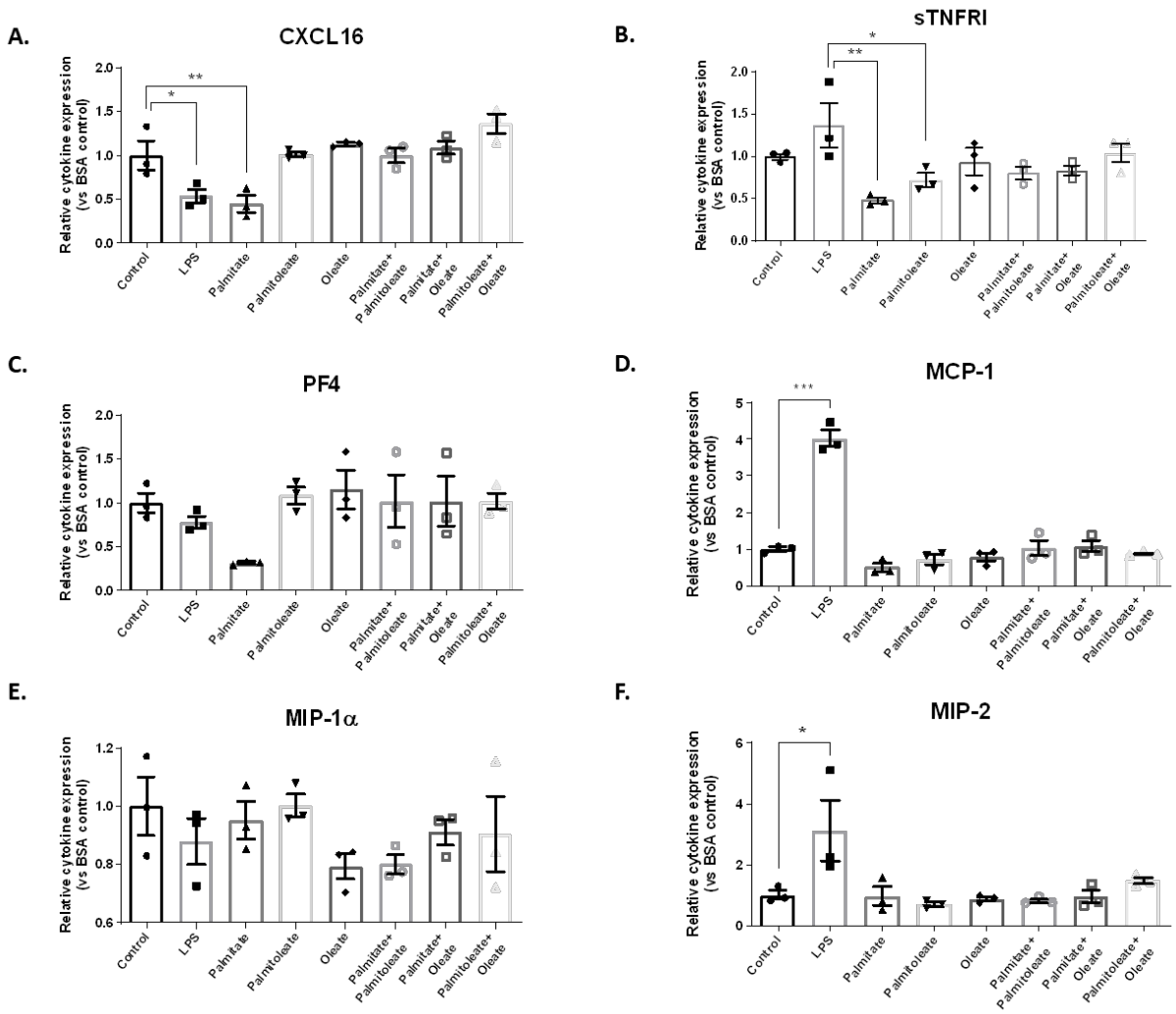


146

147 **Figure 2. Secretion of selected cytokines and chemokines in J774 media after treatment with FAs, LPS or vehicle.**

148 **A.** CXCL16. **B.** sTNRI. **C.** PF4. **D.** MCP-1. **E.** MIP-1alpha. **F.** MIP-2. Activated J774 macrophages were treated with 200

149 µM palmitate, 200 µM oleate, 200 µM palmitoleate, FA combination, 10 ng/mL LPS or control (1% w/v BSA + 0.6%

150 v/v ethanol) for 8 h. Cells were washed with PBS and fresh medium was added for 16 h. CM were collected and

151 analyzed by ELISA. Data are presented as mean ± SEM analyzed by one-way ANOVA followed by Tukey's post hoc

152 analysis (n=3 independent experiments). *p<0.05, **p<0.01, ****p<0.0001.

153 No statistically significant differences were observed for PF-4, although palmitate tended to reduce
154 secretion compared to control (1317 ± 98.45 pg/mL vs 4258 ± 822.7 pg/mL, p=0.17) and oleate (1317 ±
155 98.45 pg/mL vs 4880 ± 1636 pg/mL, p=0.06). The chemokines MIP-2 and MCP-1 were significantly
156 upregulated with LPS treatment compared to control. LPS induced a 3.1-fold increase in MIP-2 (14141 ±
157 7904 pg/mL vs 4568 ± 1202 pg/mL, p <0.05) and a 4-fold increase in MCP-1 (15476 ± 1523 pg/mL vs 3844
158 ± 367.4 pg/mL, p<0.0001). There was a trend for downregulation of MCP-1 in PA CM (1931 ± 773.1 pg/mL
159 vs 3844 ± 367.4 pg/mL, p=0.14). Finally, MIP-1α levels did not appear to be influenced by the different
160 treatments.

161 Overall, the results of these experiments revealed some trends that were similar to the results of the
162 cytokine array analysis. Importantly, CXCL16 secretion followed the same pattern, with robust
163 downregulation by palmitate and restoration to control levels with addition of UFAs. LPS also caused a
164 reduction in CXCL16 levels, whereas it strongly stimulated secretion of the chemoattractants MIP-2 and
165 MCP-1.

166

167 ### *2.3. Long-term (hours) and acute (minutes) treatment with sCXCL16 influences Akt and*
168 *ERK1/2 activation in C2C12 myotubes*

169 To test the effects CXCL16 could elicit on resident cells in skeletal muscle, differentiated C2C12 myotubes
170 were treated with sCXCL16 (1, 10, or 100 ng/mL) or control medium for 16 h and effects on Akt and ERK1/2
171 phosphorylation were examined using immunoblotting (Figure 3A). Akt activation was significantly
172 increased with all concentrations of sCXCL16 compared to control leading to a 2- to 2.4-fold upregulation
173 (2.4-fold upregulation by 1 ng/mL sCXCL16, p<0.001; 2.2-fold upregulation by 10 ng/mL sCXCL16, p<0.01;
174 2-fold upregulation by 100 ng/mL CXCL16, p<0.01 *versus* control; Figure 3B). 1 ng/mL sCXCL16 significantly

enhanced ERK1/2 phosphorylation ($p<0.05$ *versus* control; Figure 3C), while higher concentrations did not have a statistically significant effect.

High concentrations of sCXCL16 have been used consistently for *in vitro* experiments [46-53] in order to examine effects within the limitations of cell culture systems. Acute treatment with 100 ng/mL sCXCL16 had a biphasic effect on Akt activation, inducing phosphorylation at 1 minute and then, a second phase of phosphorylation at 40 and 60 minutes (Figure 3E). No significant effects were observed on the phosphorylation state of ERK1/2 (Figure 3F).

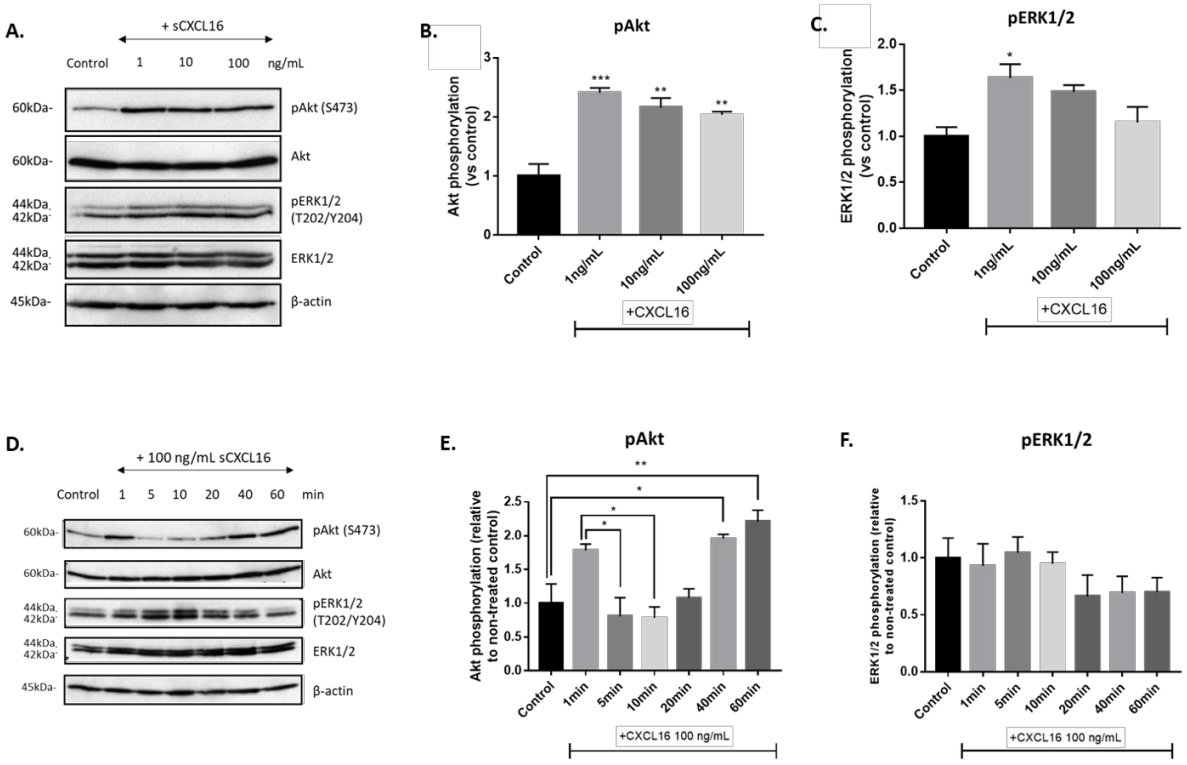


**Figure 3. Effect of acute and long-term treatment with sCXCL16 on insulin signaling pathway intermediates in C2C12 myotubes. A.** Differentiated C2C12 myotubes were treated with sCXCL16 (1, 10 or 100 ng/mL), or control for 16 h. Expression and phosphorylation of Akt and ERK1/2 were assessed using Western blotting. Representative blots of 3 independent experiments are shown. **B.** Akt phosphorylation assessed by densitometry. **C.** ERK1/2 phosphorylation assessed by densitometry. **D.** Differentiated C2C12 myotubes were treated with 100 ng/mL

sCXCL16 for the timepoints indicated. Expression and phosphorylation of Akt and ERK1/2 were assessed using Western blotting. Representative blots of 3 independent experiments are shown. **E.** Akt phosphorylation assessed by densitometry. **F.** ERK1/2 phosphorylation assessed by densitometry. B, C, E, F: Data are expressed as fold-change relative to control treatment. Data are mean ± SEM analyzed using one-way ANOVA followed by Tukey's *post hoc* analysis (n=3 independent experiments). *p<0.05, **p<0.01. ***p<0.001 *versus* control.

### *2.4. Simultaneous exposure to sCXCL16 reverses the detrimental effects of palmitate on insulin signaling and sensitivity in C2C12 myotubes*

To determine whether sCXCL16 exerts beneficial effects on insulin signaling and sensitivity, C2C12 myotubes were treated with 750 µM palmitate, 100 ng/mL sCXCL16, combination of the two factors, or control medium for 16 h and then exposed to insulin (100 nM) or vehicle (Figure 4). The expected downregulation of Akt phosphorylation (46% decrease compared to control insulin, p<0.01) was observed in myotubes exposed to palmitate (750 µM) for 16h (Figure 4B). Insulin-stimulated ERK1/2 phosphorylation was 1.9-fold higher compared to baseline control (p<0.01; Figure 4C). Simultaneous exposure to palmitate and sCXCL16 restored the insulin-stimulated phosphorylation status of Akt and ERK1/2 to control levels (p>0.05 versus control insulin). In further experiments, glycogen synthesis was used as an index of glucose disposal in C2C12 myotubes (Figure 4D). Treatment with palmitate suppressed the physiological insulin-stimulated increase in glycogen synthesis. Simultaneous treatment with sCXCL16 was able to reverse this effect, leading to a statistically significant increase in insulin-stimulated glycogen synthesis compared to baseline.

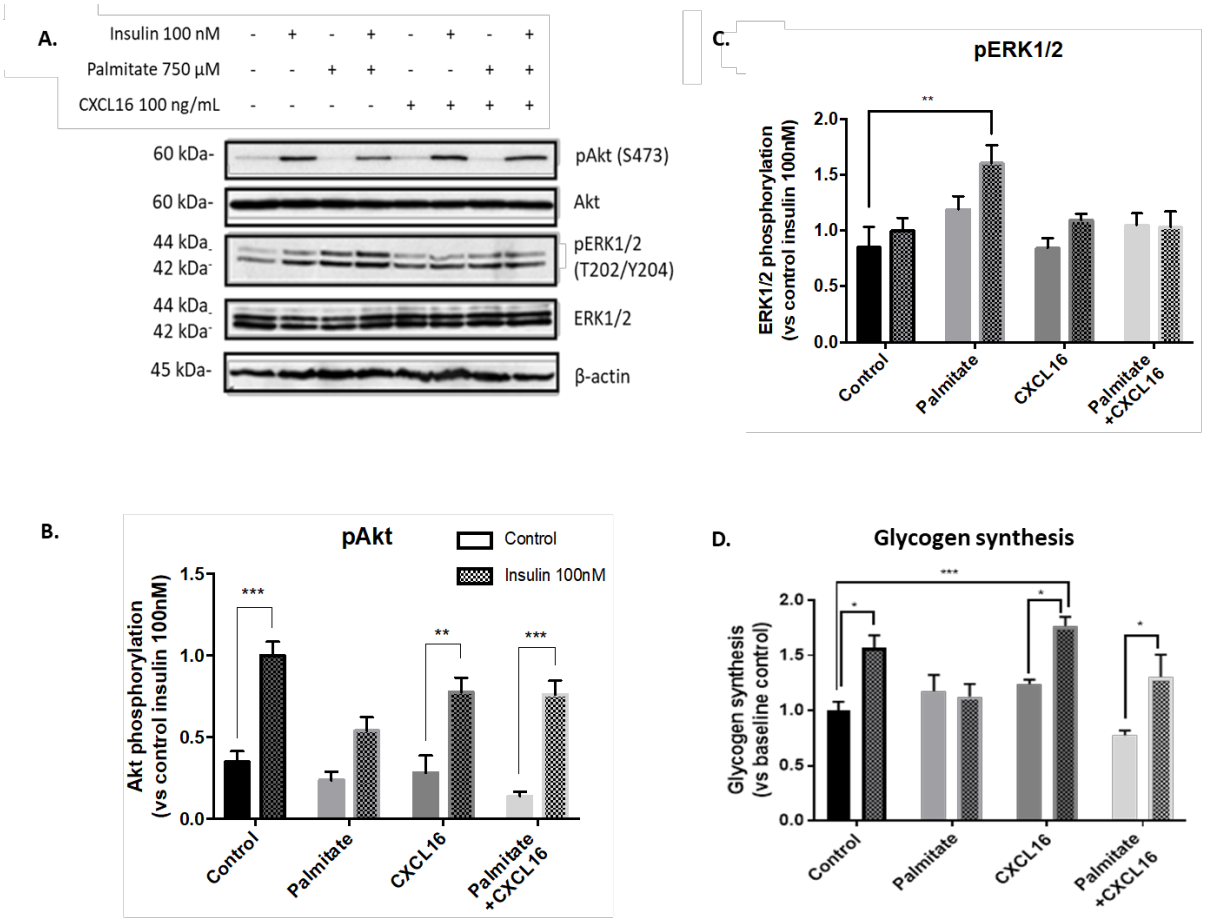


209

210 **Figure 4. Effect of sCXCL16 on insulin-stimulated phosphorylation of insulin signaling pathway intermediates and**
211 **glycogen synthesis in C2C12 myotubes.** Differentiated C2C12 myotubes were treated with 750 µM palmitate, 100
212 ng/mL sCXCL16, a combination of the two, or control medium for 16 h. Cells were then serum-starved for 2 h and
213 either glycogen synthesis assay was performed, or cells were exposed to 100 nM insulin or vehicle for 30 min.
214 Expression and phosphorylation of Akt and ERK1/2 were assessed using Western blotting. **A.** Representative blots
215 of 4 independent experiments. **B.** Akt phosphorylation assessed by densitometry. **C.** ERK1/2 phosphorylation
216 assessed by densitometry. **B, C:** Data are expressed as fold-change relative to control insulin treatment. Data are
217 shown as mean ± SEM analyzed using two-way ANOVA followed by Tukey's *post hoc* analysis (n=4 independent
218 experiments). **D.** Effect of sCXCL16 on insulin-stimulated glycogen synthesis in C2C12 myotubes. Data are expressed
219 as fold-change to baseline control treatment. Data are shown as mean ± SEM analyzed using two-way ANOVA

followed by Tukey's *post hoc* analysis (n=6 independent experiments). Filled bars: baseline samples; dotted bars: insulin-stimulated samples. *p<0.05, **p<0.01, ***p<0.001.

## 3. DISCUSSION

Cytokines and chemokines secreted by macrophages have been implicated in chemoattraction, inflammatory polarization of immune cells and enhancement or impairment of insulin sensitivity in peripheral tissues. So far, results on antagonism or genetic deletion of single cytokines in obesity and IR are inconclusive but developing successful individualized treatments targeting inflammation could prove an effective strategy for obese insulin resistant individuals who exhibit chronic low-grade inflammation. In the studies described in this paper, CM from macrophages treated with palmitate and palmitate + palmitoleate were screened with a cytokine array to examine differential expression and the results were followed-up in additional experiments analyzed using specific ELISAs. Interestingly, secretion of a relatively recently described chemokine, CXCL16, was strongly downregulated by both palmitate and LPS treatment.

CXCL16 has been associated with atherosclerosis and cardiovascular disease [54-56] as well as cancer [57], and is considered mainly pro-inflammatory. It exists in two forms, soluble and transmembrane, and both forms are expressed by macrophages [58]. The literature so far has mainly focused on the chemoattractant, proliferative and scavenging properties of CXCL16 in inflammatory diseases and cancer. A few publications have investigated CXCL16 in the context of metabolic disease [59-63], but there is no data concerning its possible action on resident tissue cells in insulin-sensitive tissues such as skeletal muscle. The only known receptor for CXCL16, CXCR6, is a class A G-protein-coupled receptor [64, 65], with preferential coupling to $G_{i/o}$ proteins [65]. Studies investigating atherosclerosis development, angiogenesis or cancer progression have indicated that CXCL16 can activate components of the PI3K/Akt

243 pathway and other signaling elements that might be of interest in the context of IR. A study by
244 Chandrasekar et al. showed that CXCL16 acts through CXCR6 to induce NF-κB activation in aortic smooth
245 muscle cells via G proteins, but also stimulates PI3K and Akt activation. Downstream of Akt, GSK3α/β
246 phosphorylation was also increased by CXCL16 treatment [46]. CXCL16 promotes growth, migration and
247 tube formation by human umbilical vein endothelial cells (HUVEC) through activation of Akt, but also p38
248 MAPK and ERK1/2 [66]. ERK1/2 has also been implicated as a mediator of CXCL16-induced angiogenic
249 effects in HUVEC [67]. Moreover, in liver carcinoma cells, CXCL16 treatment upregulated Akt and ERK1/2
250 activities, which are associated with invasion and metastasis regulation [68].

251 CXCR6 expression by myotubes (murine C2C12 cells) has previously been reported [69-71]. Since the
252 secretion of soluble CXCl16 was downregulated by both palmitate and LPS treatment, it was intriguing to
253 examine its potential role in obesity and IR. As CXCL16 has been shown to act upstream of Akt and ERK1/2,
254 it is possible that it could influence insulin signaling and sensitivity by modulating these intermediates. In
255 C2C12 myotubes, acute and longer-term treatment with sCXCL16 were able to increase basal Akt
256 phosphorylation in the absence of insulin. Although long-term treatment with sCXCL16 did not have an
257 additional effect compared to control upon insulin stimulation, simultaneous treatment with palmitate
258 was able to restore insulin-stimulated Akt phosphorylation and suppress ERK1/2 phosphorylation to
259 control levels. In addition to regulating Akt, a major intermediate of the PI3K pathway, the suppression of
260 ERK1/2 by sCXCL16 is also of interest as high levels of activation can impair insulin sensitivity in myocytes
261 [72-74]. Importantly, dietary glucose is mainly stored in muscle cells in the form of glycogen rendering
262 glycogen synthesis a major route for glucose disposal in skeletal muscle [75]. Thus, to assess effects on
263 insulin-stimulated glucose utilization in C2C12 myotubes, measurements of glycogen synthesis were
264 carried out. Co-administration of sCXCL16 opposed against the deleterious effects of palmitate on insulin-

stimulated glycogen synthesis. These results suggest that sCXCL16 could hold a protective role for myotube insulin sensitivity in an environment of high palmitate concentration.

CXCL16 and CXCR6 mRNA expression was detected in C2C12 myotubes by qPCR (Supplementary Figure 4). It would also be pertinent to examine in future studies if CXCL16 is produced by primary human myotubes and adipocytes under different conditions associated with IR. For example, the effects of CM derived from macrophages exposed to TNF-α, LPS and other inflammatory molecules, as well as FA on secretion of CXCL16 from resident cells could be investigated in future studies. In addition, since there is evidence that CXCL16 correlates with M2 macrophage polarization [76, 77] and infiltration [78], the effects of sCXCL16 on the polarization of resident macrophages isolated from skeletal muscle and AT of lean and obese human participants would be of particular relevance. Investigations such as these could shed light on the potential effects of CXCL16 on macrophage polarization in the context of obesity and IR in peripheral tissues.

To the author's knowledge, no other chemokine or cytokine has direct protective effects on insulin signaling and glycogen synthesis through Akt activation. IL-15 has been found to increase glucose uptake by muscle cells via STAT3 (Signal Transducer And Activator Of Transcription 3) [79], but there are varied results in the literature. Some studies have reported anti-inflammatory actions of IL-15 and beneficial metabolic effects through stimulation of weight loss and energy expenditure [80]. Additionally, treatment of cultured adipocytes with IL-15 led to inhibition of FA synthase and lipid accumulation [81] and genetic IL-15 deficiency promoted adaptive thermogenesis and reduced pro-inflammatory mediators in AT [82]. IL-6 has also been reported to acutely stimulate insulin sensitivity and enhance glucose uptake, while inhibiting inflammation. However, chronically it can induce IR and promote inflammation in peripheral tissues [83]. A recent paper attributed opposing roles regarding macrophage accumulation to IL-6 secreted by myeloid cells *versus* resident cells (adipocytes and myocytes), adding to the complexity of

cytokine-mediated inflammatory responses in metabolic disease [84]. Findeisen et al. provided a path to manipulate downstream responses with the use of a 'designer cytokine' [19], proving that such next-generation pharmacological agents, preferentially harnessing beneficial effects of inflammatory components, could hold promise for T2D treatment.

Although CXCL16 secretion has the potential to influence insulin signaling in tissue resident cells, the chemoattractant properties of sCXCL16 should not be overlooked. CXCL16 is a chemoattractant for natural killer (NK) [85] and natural killer T (NKT) cells [86-89]. Thus, CXCL16 might chemoattract NK and NKT cells that in turn could activate macrophages, as they secrete different cytokines, such as TNF-α and IFN-γ [90]. Wang et al. demonstrated the potential for another interesting interaction as trophoblast-derived sCXCL16 induces M2 macrophage polarization that in turn inactivates NK cells at the maternal–fetal interface [76]. CXCL16 secretion could also affect macrophage and neutrophil chemoattraction, adding to the milieu of potential roles CXCL16 could play in AT and skeletal muscle inflammation in obesity.

## *Conclusions*

The effects of sCXCL16 on myotube insulin signaling and sensitivity have not previously been reported in the literature. In this study, a consistent stimulatory effect on Akt activation, a key component of the insulin signaling pathway, was evident in C2C12 myotubes, with both an acute and a longer-term effect in the basal state observed. sCXCL16 was able to reverse the detrimental effects of palmitate on insulin-stimulated Akt activation and glycogen synthesis (Figure 5). These data propose a putative role of sCXCL16 in regulating insulin signaling in myotubes that warrants further investigation in future *in vitro* and *in vivo* studies.

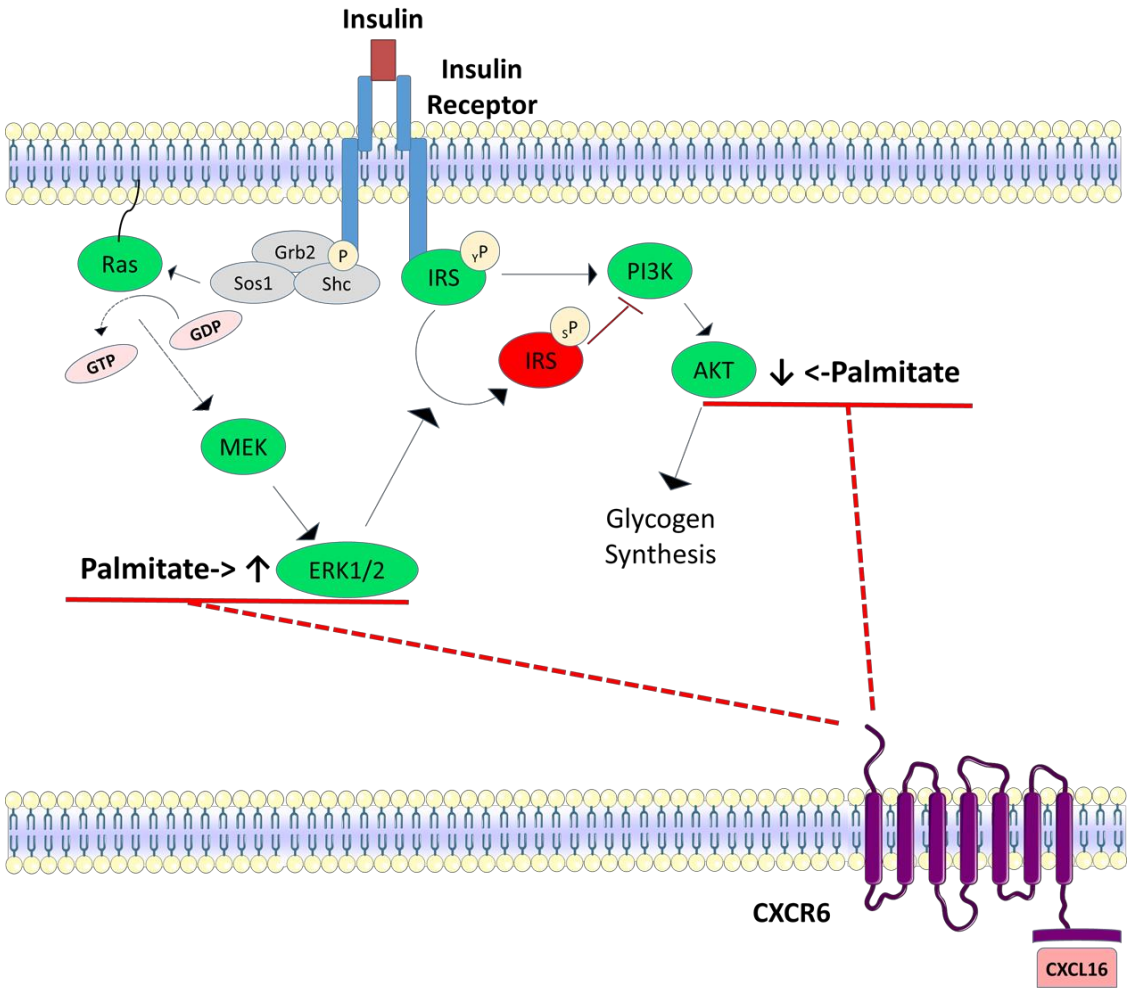


309

310 **Figure 5. CXCL16 preserves Akt activation and glycogen synthesis in palmitate-treated myotubes.** Palmitate
311 treatment compromises myotube insulin signaling and sensitivity. Simultaneous treatment with CXCL16 preserves
312 insulin-stimulated glycogen synthesis by maintaining Akt activation and downregulating ERK1/2 phosphorylation.
313 Akt: protein kinase B/Akt, ERK1/2: extracellular regulated kinases 1/2, Grb2: growth factor receptor-bound protein
314 2, GDP: guanosine diphosphate, GTP: guanosine triphosphate, IRS: insulin receptor substrate, MEK: Mitogen-
315 activated protein kinase kinase, PI3K: phosphoinositide 3-kinase, Shc: Src homology 2 domain containing
316 transforming protein, Sos1: son of sevenless homologue 1. SP: serine phosphorylation, YP: tyrosine phosphorylation.

# 4. MATERIALS AND METHODS

## *4.1. Maintenance of cell lines*

J774A.1 cells (referred to as J774) and C2C12 cells were purchased from the American Type Culture Collection and maintained in high glucose (25 mM) Dulbecco's Modified Eagle Medium (DMEM) with GlutaMAX supplement with added 10% v/v heat-inactivated fetal bovine serum (FBS) and 1% v/v antibiotic-antimycotic (ABAM) mixture. Cells were maintained at 37°C in 5% CO2 in a humidified tissue culture incubator. Cells were maintained in 20 mL growth medium in T175 cell culture flasks and passaged as required, in the case of C2C12, before cell confluence reached more than 70% (usually every 2-3 days) to avoid spontaneous differentiation.

## *4.2. C2C12 differentiation into myotubes*

C2C12 myoblasts were detached from flasks using Trypsin-EDTA, counted and seeded into plates at a density of $2x10^5$ cells/mL. When 100% confluence was reached (the next day), differentiation into myotubes was induced by changing to differentiation medium consisting of DMEM supplemented with 2% v/v heat-inactivated HS and 1% v/v ABAM for 5 days before use. Media were replaced every 2 days during differentiation. Treatments were routinely added on the afternoon of day 5 of differentiation when fusion of myoblasts to form elongated myotubes had been achieved.

## *4.3. Fatty acid treatments*

FAs, specifically the SFA palmitate and the UFAs palmitoleate and oleate, used for treatments were conjugated to FA-free fraction V BSA to mimic their presence in their blood *in vivo*, where they are bound to serum albumin [91]. 1-2% w/v BSA (depending on the final FA concentration, specifically 1% w/v for

200 µM, 1.5% w/v for 500 µM and 2% w/v for 750 µM) was added to pre-warmed growth medium and left to mix on a laboratory roller for 30 min. 75 mM palmitic acid, palmitoleic acid and oleic acid stock solutions were prepared in 100% ethanol. Palmitic acid solutions were always prepared fresh, while palmitoleic and oleic acid stocks were stored at -20°C. Appropriate volumes of stock solutions were added to growth medium containing BSA to give the final concentrations indicated, mixed and heated to 40°C in a water bath with occasional manual mixing for 30 min to allow conjugation of FAs with BSA. For control treatment, an equal amount of ethanol without FAs was added to growth medium containing BSA and incubated alongside the FA media. The media were filter-sterilised before addition to the cells.

### *4.4. Generation of conditioned media*

Activated J774 cells were treated for 8 h with growth medium containing 1.5% w/v FA-free fraction V BSA conjugated with FAs, prepared as described in 2.1.5. Cells were also exposed to growth medium containing LPS 10 ng/mL (positive control) and to control treatments (1.5% w/v BSA + ethanol and growth medium without BSA). Treatments were removed, cells washed with PBS, and fresh medium added for 16 h. CM were collected, centrifuged at 200 x *g* for 5 min at RT, and the supernatant was transferred to a fresh tube and subsequently, added to differentiated C2C12 myotubes for 16 h [31].

### *4.5. Cytokine array*

J774 cells were seeded at $1.5 \times 10^5$ cells/mL in T175 flasks and activated using 200 ng/mL PMA. 3 days after, cells were treated with growth medium containing 1.5% FA-free fraction V BSA and 500 µM palmitate, 500 µM palmitate + 500 µM palmitoleate, or control (1.5% w/v BSA + 0.66% v/v ethanol). After 8 h, cells were washed three times with PBS and fresh medium added for 16 h to generate CM. This was collected and used immediately for the mouse cytokine array.

The RayBiotech mouse cytokine antibody array C3 (for cytokine array map, see Supplementary Figure 1) was used according to the supplier's instructions to detect levels of 62 cytokines in J774 CM. The antibody array membranes and kit components were equilibrated to RT before 2mL of blocking buffer were added to the membrane and incubated for 30 min. Blocking buffer was aspirated and 2mL of CM was added per membrane and incubated for 3 h at RT. The CM were aspirated and 3 x 5-min washes with 1X Wash Buffer I followed by 2 x 5-min washes with 1X Wash Buffer II were performed. 1 mL of the Biotinylated Antibody Cocktail was added to each membrane and incubated for 2 h at RT. The antibody cocktail was aspirated and 3 x 5-min washes with 1X Wash Buffer I followed by 2 x 5-min washes with 1X Wash Buffer II were performed. 2 mL of 1X HRP-Streptavidin were added to each membrane and incubated for 2 h at RT. After aspiration, 3 washes 5 min each with 1X Wash Buffer I followed by 2 washes 5 min each with 1X Wash Buffer II were performed. Membranes were placed onto a plastic sheet and 500 µl of the Detection Buffer mixture (equal volumes 1:1 of Detection Buffer C and Detection Buffer D) were added onto each membrane and incubated for 2 min at RT. Another plastic sheet was placed on top of the membranes so that the membrane was enclosed between the two sheets.

Membranes were exposed to X-ray film and the Gilles Carpentier dot blot analyzer for Image J (Image J 1.42q, National Institutes of Health, USA) was used to obtain mean signal density from scanned blots. The following equation was used to calculate signal intensity, which was normalized to the control treatment membrane to account for exposure variability:

**X(Ny) = X(y) * P1/P(y)**

where: X(Ny)= normalized signal intensity for spot "X" on Array "y", X(y) = mean signal density for spot "X" on Array for sample "y", P1 = mean signal density of Positive Control spots on reference array (control treatment), and P(y) = mean signal density of Positive Control spots on Array "y"

### *4.6. ELISAs*

Enzyme-linked immunosorbent assay (ELISA) was used to verify the results of the cytokine array for selected cytokines (CXCL16, MCP-1, MIP-1 alpha, MIP-2, sTNFRI, and PF-4) and to test additional treatments. J774 cells were seeded at $1.5x10^5$ cells/mL in T175 flasks and activated using 200 ng/mL PMA. 3 days later, cells were treated with growth medium containing 1% w/v FA-free fraction V BSA and 200 µM palmitate, 200 µM palmitoleate, 200 µM palmitate + 200 µM palmitoleate, 200 µM oleate, 200 µM palmitate + 200 µM oleate, 200 µM oleate + 200 µM palmitoleate, or control (1% w/v BSA+ 0.6% v/v ethanol). After 8 h, cells were washed three times with PBS and fresh medium added for 16 h to generate CM. CM was collected and stored at -80$^{o}$C until 3 repeats were obtained.

RayBio Mouse ELISA kits were used according to the manufacturer's instructions. CM samples were thawed on ice on the day of the assay. 96-well plates coated with antibodies against the target cytokines were provided and 100 µL standards and samples were pipetted into wells. The plates were incubated for 2.5 h at RT with gentle shaking to allow target cytokines present in the samples and standards to bind specifically to the immobilized antibody. Wells were washed 4 times with 300 µL 1X Wash Buffer and 100 µL biotinylated antibody against the host species of the primary antibody was added for 1 h at RT with gentle shaking. Wells were washed 4 times with 300 µL 1X Wash Buffer and 100 µL HRP-conjugated streptavidin solution was added for 45 min at RT with gentle shaking. After 4 washes, 100 µl of 3,3,5,5'-tetramethylbenzidine substrate reagent were added, the plates were covered with foil and incubated for 30 min at RT with gentle shaking. Color development is proportional to bound cytokines. 50 µL of stop solution (0.2M sulfuric acid) were added to each well. The acidic conditions deactivate enzymatic activity and change the color from blue to yellow. Plates were read immediately at 450 nm using a Tecan Pro2000 plate reader.

406 The mean absorbance for each set of duplicated standards, controls and samples was calculated and the
407 average optical density (OD) of the blank standard (0.0 pg/mL) was subtracted. The standard curve was
408 generated using GraphPad Prism (Version 7.02, GraphPad Software, Inc.). Log(concentration) was plotted
409 on the x axis and log(OD) on the y axis, and the best-fit straight line was drawn. Sample concentration was
410 extrapolated via the resulting equation, results were copied to Excel (Microsoft Office 2016, Microsoft,
411 US) and calculations were made using control treatment (BSA + ethanol) as a reference.

412

413 *4.7. Immunoblotting*

414 Myotubes were lysed in radioimmunoprecipitation assay (RIPA) buffer, homogenized using an Ultra-
415 Turrax (IKA; Staufen, Germany) and denatured in Laemmli buffer for 10 min at 65 °C. Proteins were
416 resolved by SDS–PAGE, electro-transferred and immunoblotted as previously described (Patel et al.,
417 2012). After the completion of transfer, membranes were either stored at 4°C in Tris-buffered saline (TBS)
418 (136.9 mM NaCl, 2.7 mM KCl, 12.4 mM Tris, pH 7.4), containing 0.1% v/v Tween-20 (TBST) until further
419 use or briefly washed in TBST and incubated with block solution for 1 h at RT to eliminate non-specific
420 binding of antibodies. Block solutions were either 5% w/v milk in TBST or 5% w/v BSA in TBST as indicated
421 in Table 2.3. Subsequently, membranes were incubated with primary antibodies diluted in primary
422 antibody dilution buffer (TBST containing 2% w/v BSA, 0.5% w/v phenol red and 0.02% w/v sodium azide).
423 Incubation took place on a laboratory orbital shaker or roller mixer at 4°C for 16 h overnight, with the
424 exception of the β-actin antibody that was incubated for 2 h at RT. Details for the antibodies used are
425 provided at Table 1.

426 Following primary antibody incubation, membranes were washed in wash buffer (TBST containing
427 additional 0.36 M NaCl to achieve thorough washing) three times for 5 min each. Horseradish peroxidase
428 (HRP)-conjugated secondary antibody against the host species in which the primary antibody was raised

was incubated for 1 h at RT. The secondary antibodies were diluted 1:10,000 in TBST containing 5% w/v milk. After 1 h, three washes in wash buffer for 5 min each and one wash in TBS followed.

Washed membranes were incubated with 0.5-1 mL (enough to cover the surface of the membrane) of ECL reagent (Enhanced Luminol Reagent Plus: Oxidizing Reagent Plus, 1:1 ratio, PerkinElmer) for 1 min prior to visualization of the bands. Detection of proteins was achieved by exposing membranes to a light-sensitive X-ray film (Super RX, FujiFilm, Bedford, UK) in a cassette for periods ranging from 1 s to 15 min. Films were scanned and quantified using the open-source software ImageJ (National Institutes of Health, Bethesda, Maryland, USA). β-actin was used as a loading control.

**Table 1. Primary antibodies (Ab) used for Western Blotting**

| Primary Ab | Supplier | Catalogue number | Molecular Weight (kDa) | Host species | Dilution in primary Ab Buffer | Block Buffer | Primary Ab Incubation |
|---|---|---|---|---|---|---|---|
| ***Akt*** | Cell Signaling Technology | 9272S | 60 | rabbit | 1:1,000 | 5% w/v milk in TBST | 16 h, 4°C |
| ***β-actin*** | Merck (Sigma-Aldrich) | A2228 | 42 | mouse | 1:2,000 | 5% w/v milk in TBST | 2 h, RT |
| ***ERK1 (K-23)*** | Santa Cruz | sc-94 | 44 | rabbit | 1:1,000 | 5% w/v milk in TBST | 16 h, 4°C |
| ***p-Akt (D9E)-XP (Ser473)*** | Cell Signaling Technology | 4060S | 60 | rabbit | 1:1,000 | 5% w/v BSA in TBST | 16 h, 4°C |
| ***p-ERK1/2 (Thr202 /Tyr 204)*** | Cell Signaling Technology | 9101S | 44/42 | rabbit | 1:2,000 | 5% w/v BSA in TBST | 16 h, 4°C |

Akt: Protein Kinase B, ERK: extracellular regulated kinases.

### *4.8. Glycogen Synthesis assays*

Incorporation of glucose into glycogen in myotubes was measured by modifying a published protocol [92]. Following appropriate treatments as indicated in subsequent chapters, media were aspirated, C2C12 myotubes were washed twice with PBS and then, treated with low glucose (5.55 mM) DMEM + 1% v/v

ABAM and no serum for 2 h. Following this, 2 µCi D-[U-14C]-glucose ± 100 nM insulin was added per well for 1 h at 37°C. The reaction was terminated by washing 3 times with ice-cold PBS. Myotubes were lysed in 450 µL/well Radio-Immuno-Precipitation Assay (RIPA) Buffer [65 mM Tris, 150 mM NaCl, 5 mM EDTA (pH 7.4), 1% v/v Igepal-CA630 detergent, 0.5% w/v sodium deoxycholate, 0.1% w/v sodium dodecyl sulfate (SDS), 10% v/v glycerol] and lysates heated at 100°C for 10 min. The lysates were homogenized using a 19-gauge needle and syringe. 300 µL of lysate was added to a fresh tube with 600 µL 100% ice-cold ethanol and unlabeled glycogen powder (for glycogen pellet visualization purposes). The remaining lysate was stored at -20°C for measurement of total protein content using a bicinchoninic acid assay (BCA) according to the manufacturer's protocol (described in 2.3.2). Glycogen was precipitated in ethanol at 4°C overnight, then at -20°C for 30 min, before centrifugation at 13,000 g for 20 min. The pellet was dissolved in 100 µL distilled water, heated at 60°C for 20 min to facilitate resuspension, mixed with 5 mL scintillant and counted using a Tricarb 2810TR Liquid Scintillation Analyzer running on QuantaSmart software (Perkin Elmer Life and Analytical Sciences). Results were calculated as pmol/(min*mg of protein).

### *4.9. Statistical analysis*

Data were analyzed using GraphPad Prism (Version 7.02, GraphPad Software, US). Results from more than two unrelated groups were analyzed using analysis of variance (ANOVA). Statistical analysis involving paired treatments was performed using two-way ANOVA for three or more groups. Statistical tests used are indicated within the text and at figure legends. If significance was found using one-way or two-way ANOVA, the *post-hoc* Tukey's multiple comparisons test was applied to detect statistically significant differences between groups. The number of biological repeats is indicated in the figure legends. A p-value below 0.05 was considered significant.

## Acknowledgements

This work was supported by funding available at the Comparative Biomedical Sciences Department, Royal Veterinary College. I would like to thank Professor Caroline Wheeler-Jones and Dr Mark Cleasby for their guidance and support during my PhD studies.

## REFERENCES

1. WHO. *Obesity and overweight fact sheet*. 2017.
2. WHO. *Diabetes fact sheet.* 2017.
3. Lebovitz, H.E., *Insulin resistance: definition and consequences.* Exp Clin Endocrinol Diabetes, 2001. **109 Suppl 2**: p. S135-48.
4. Hardy, O.T., M.P. Czech, and S. Corvera, *What causes the insulin resistance underlying obesity?* Curr Opin Endocrinol Diabetes Obes, 2012. **19**(2): p. 81-7.
5. Taylor, R., *Insulin resistance and type 2 diabetes.* Diabetes, 2012. **61**(4): p. 778-9.
6. Martin, B.C., et al., *Role of glucose and insulin resistance in development of type 2 diabetes mellitus: results of a 25-year follow-up study.* Lancet, 1992. **340**(8825): p. 925-9.
7. Olefsky, J.M. and C.K. Glass, *Macrophages, inflammation, and insulin resistance.* Annu Rev Physiol, 2010. **72**: p. 219-46.
8. Huber, J., et al., *CC chemokine and CC chemokine receptor profiles in visceral and subcutaneous adipose tissue are altered in human obesity.* J Clin Endocrinol Metab, 2008. **93**(8): p. 3215-21.
9. Yamakawa, T., et al., *Augmented production of tumor necrosis factor-alpha in obese mice.* Clin Immunol Immunopathol, 1995. **75**(1): p. 51-6.
10. Hotamisligil, G.S., N.S. Shargill, and B.M. Spiegelman, *Adipose expression of tumor necrosis factor-alpha: direct role in obesity-linked insulin resistance.* Science, 1993. **259**(5091): p. 87-91.
11. Weisberg, S.P., et al., *Obesity is associated with macrophage accumulation in adipose tissue.* J Clin Invest, 2003. **112**(12): p. 1796-808.
12. Xu, H., et al., *Chronic inflammation in fat plays a crucial role in the development of obesity-related insulin resistance.* J Clin Invest, 2003. **112**(12): p. 1821-30.
13. Cinti, S., et al., *Adipocyte death defines macrophage localization and function in adipose tissue of obese mice and humans.* J Lipid Res, 2005. **46**(11): p. 2347-55.
14. Prieur, X., et al., *Differential lipid partitioning between adipocytes and tissue macrophages modulates macrophage lipotoxicity and M2/M1 polarization in obese mice.* Diabetes, 2011. **60**(3): p. 797-809.
15. Fink, L.N., et al., *Pro-inflammatory macrophages increase in skeletal muscle of high fat-fed mice and correlate with metabolic risk markers in humans.* Obesity (Silver Spring), 2014. **22**(3): p. 747-57.
16. Weisberg, S.P., et al., *CCR2 modulates inflammatory and metabolic effects of high-fat feeding.* J Clin Invest, 2006. **116**(1): p. 115-24.
17. Patsouris, D., et al., *Insulin resistance is associated with MCP1-mediated macrophage accumulation in skeletal muscle in mice and humans.* PLoS One, 2014. **9**(10): p. e110653.

18. Inouye, K.E., et al., *Absence of CC chemokine ligand 2 does not limit obesity-associated infiltration of macrophages into adipose tissue.* Diabetes, 2007. **56**(9): p. 2242-50.
19. Findeisen, M., et al., *Treatment of type 2 diabetes with the designer cytokine IC7Fc.* Nature, 2019. **574**(7776): p. 63-68.
20. Fink, L.N., et al., *Expression of anti-inflammatory macrophage genes within skeletal muscle correlates with insulin sensitivity in human obesity and type 2 diabetes.* Diabetologia, 2013. **56**(7): p. 1623-8.
21. Khan, I.M., et al., *Intermuscular and perimuscular fat expansion in obesity correlates with skeletal muscle T cell and macrophage infiltration and insulin resistance.* Int J Obes (Lond), 2015. **39**(11): p. 1607-18.
22. Varma, V., et al., *Muscle inflammatory response and insulin resistance: synergistic interaction between macrophages and fatty acids leads to impaired insulin action.* Am J Physiol Endocrinol Metab, 2009. **296**(6): p. E1300-10.
23. Thiebaud, D., et al., *The effect of graded doses of insulin on total glucose uptake, glucose oxidation, and glucose storage in man.* Diabetes, 1982. **31**(11): p. 957-63.
24. Turner, N., et al., *Fatty acid metabolism, energy expenditure and insulin resistance in muscle.* J Endocrinol, 2014. **220**(2): p. T61-79.
25. Reaven, G.M., et al., *Measurement of plasma glucose, free fatty acid, lactate, and insulin for 24 h in patients with NIDDM.* Diabetes, 1988. **37**(8): p. 1020-4.
26. Pussinen, P.J., et al., *Endotoxemia is associated with an increased risk of incident diabetes.* Diabetes Care, 2011. **34**(2): p. 392-7.
27. Boutagy, N.E., et al., *Metabolic endotoxemia with obesity: Is it real and is it relevant?* Biochimie, 2016. **124**: p. 11-20.
28. Rastelli, M., C. Knauf, and P.D. Cani, *Gut Microbes and Health: A Focus on the Mechanisms Linking Microbes, Obesity, and Related Disorders.* Obesity (Silver Spring), 2018. **26**(5): p. 792-800.
29. Ghanim, H., et al., *Increase in plasma endotoxin concentrations and the expression of Toll-like receptors and suppressor of cytokine signaling-3 in mononuclear cells after a high-fat, high-carbohydrate meal: implications for insulin resistance.* Diabetes Care, 2009. **32**(12): p. 2281-7.
30. Pardo, V., et al., *Opposite Cross-Talk by Oleate and Palmitate on Insulin Signaling in Hepatocytes through Macrophage Activation.* J Biol Chem, 2015.
31. Talbot, N.A., C.P. Wheeler-Jones, and M.E. Cleasby, *Palmitoleic acid prevents palmitic acid-induced macrophage activation and consequent p38 MAPK-mediated skeletal muscle insulin resistance.* Mol Cell Endocrinol, 2014. **393**(1-2): p. 129-42.
32. Kratz, M., et al., *Metabolic dysfunction drives a mechanistically distinct proinflammatory phenotype in adipose tissue macrophages.* Cell Metab, 2014. **20**(4): p. 614-25.
33. Shi, H., et al., *TLR4 links innate immunity and fatty acid-induced insulin resistance.* J Clin Invest, 2006. **116**(11): p. 3015-25.
34. Nasimian, A., et al., *Protein tyrosine phosphatase 1B (PTP1B) modulates palmitate-induced cytokine production in macrophage cells.* Inflamm Res, 2013. **62**(2): p. 239-46.
35. Nakakuki, M., et al., *Eicosapentaenoic acid suppresses palmitate-induced cytokine production by modulating long-chain acyl-CoA synthetase 1 expression in human THP-1 macrophages.* Atherosclerosis, 2013. **227**(2): p. 289-96.
36. Huynh, K., et al., *Lipidomic Profiling of Murine Macrophages Treated with Fatty Acids of Varying Chain Length and Saturation Status.* Metabolites, 2018. **8**(2).
37. Riera-Borrull, M., et al., *Palmitate Conditions Macrophages for Enhanced Responses toward Inflammatory Stimuli via JNK Activation.* J Immunol, 2017. **199**(11): p. 3858-3869.
38. Kewalramani, G., et al., *Palmitate-activated macrophages confer insulin resistance to muscle cells by a mechanism involving protein kinase C theta and epsilon.* PLoS One, 2011. **6**(10): p. e26947.

39. Samokhvalov, V., et al., *Palmitate- and lipopolysaccharide-activated macrophages evoke contrasting insulin responses in muscle cells.* Am J Physiol Endocrinol Metab, 2009. **296**(1): p. E37-46.
40. de Alvaro, C., et al., *Tumor necrosis factor alpha produces insulin resistance in skeletal muscle by activation of inhibitor kappaB kinase in a p38 MAPK-dependent manner.* J Biol Chem, 2004. **279**(17): p. 17070-8.
41. Chan, K.L., et al., *Palmitoleate Reverses High Fat-induced Proinflammatory Macrophage Polarization via AMP-activated Protein Kinase (AMPK).* J Biol Chem, 2015. **290**(27): p. 16979-88.
42. Cen, H., et al., *Multiplex epitope detection: a new method overcomes limitations of antibody arrays.* Proteomics, 2013. **13**(10-11): p. 1696-700.
43. Kodadek, T., *Protein microarrays: prospects and problems.* Chem Biol, 2001. **8**(2): p. 105-15.
44. Sanchez-Carbayo, M., *Antibody arrays: technical considerations and clinical applications in cancer.* Clin Chem, 2006. **52**(9): p. 1651-9.
45. IUIS/WHO, *International Union of Immunological Societies/World Heatlh Organisation subcomittee on chemokine nomenclature: Chemokine/chemokine receptor nomenclature.* J Leukoc Biol, 2001. **70**(3): p. 465-6.
46. Chandrasekar, B., S. Bysani, and S. Mummidi, *CXCL16 signals via Gi, phosphatidylinositol 3-kinase, Akt, I kappa B kinase, and nuclear factor-kappa B and induces cell-cell adhesion and aortic smooth muscle cell proliferation.* J Biol Chem, 2004. **279**(5): p. 3188-96.
47. Hu, W., et al., *CXCL16 and CXCR6 are coexpressed in human lung cancer in vivo and mediate the invasion of lung cancer cell lines in vitro.* PLoS One, 2014. **9**(6): p. e99056.
48. Borst, O., et al., *The inflammatory chemokine CXC motif ligand 16 triggers platelet activation and adhesion via CXC motif receptor 6-dependent phosphatidylinositide 3-kinase/Akt signaling.* Circ Res, 2012. **111**(10): p. 1297-307.
49. Diegelmann, J., et al., *Expression and regulation of the chemokine CXCL16 in Crohn's disease and models of intestinal inflammation.* Inflamm Bowel Dis, 2010. **16**(11): p. 1871-81.
50. Day, C., et al., *The chemokine CXCL16 is highly and constitutively expressed by human bronchial epithelial cells.* Exp Lung Res, 2009. **35**(4): p. 272-83.
51. Huang, Y., et al., *Chemokine CXCL16, a scavenger receptor, induces proliferation and invasion of first-trimester human trophoblast cells in an autocrine manner.* Hum Reprod, 2006. **21**(4): p. 1083-91.
52. Lu, Y., et al., *CXCL16 functions as a novel chemotactic factor for prostate cancer cells in vitro.* Mol Cancer Res, 2008. **6**(4): p. 546-54.
53. Schramme, A., et al., *The role of CXCL16 and its processing metalloproteinases ADAM10 and ADAM17 in the proliferation and migration of human mesangial cells.* Biochem Biophys Res Commun, 2008. **370**(2): p. 311-6.
54. Ma, A., et al., *Elevation of serum CXCL16 level correlates well with atherosclerotic ischemic stroke.* Arch Med Sci, 2014. **10**(1): p. 47-52.
55. Lv, Y., et al., *Associations of CXCL16/CXCR6 with carotid atherosclerosis in patients with metabolic syndrome.* Clin Nutr, 2013. **32**(5): p. 849-54.
56. Lehrke, M., et al., *CXCL16 is a marker of inflammation, atherosclerosis, and acute coronary syndromes in humans.* J Am Coll Cardiol, 2007. **49**(4): p. 442-9.
57. Deng, L., et al., *CXCR6/CXCL16 functions as a regulator in metastasis and progression of cancer.* Biochim Biophys Acta, 2010. **1806**(1): p. 42-9.
58. Shimaoka, T., et al., *Cell surface-anchored SR-PSOX/CXC chemokine ligand 16 mediates firm adhesion of CXC chemokine receptor 6-expressing cells.* J Leukoc Biol, 2004. **75**(2): p. 267-74.
59. Kurki, E., et al., *Distinct effects of calorie restriction on adipose tissue cytokine and angiogenesis profiles in obese and lean mice.* Nutr Metab (Lond), 2012. **9**(1): p. 64.

60. Mayi, T.H., et al., *Human adipose tissue macrophages display activation of cancer-related pathways.* J Biol Chem, 2012. **287**(26): p. 21904-13.
61. Fenton, J.I., et al., *Diet-induced adiposity alters the serum profile of inflammation in C57BL/6N mice as measured by antibody array.* Diabetes Obes Metab, 2009. **11**(4): p. 343-54.
62. Ribeiro, S.M., et al., *CXCL-16, IL-17, and bone morphogenetic protein 2 (BMP-2) are associated with overweight and obesity conditions in middle-aged and elderly women.* Immun Ageing, 2017. **14**: p. 6.
63. Santiago-Fernandez, C., et al., *Msr1 and Cxcl16 scavenger receptors in adipose tissue are positively associated with BMI and insulin resistance*, in *18th European Congress of Endocrinology*. 2016: Munich, Germany. p. EP803.
64. Koenen, A., et al., *The DRF motif of CXCR6 as chemokine receptor adaptation to adhesion.* PLoS One, 2017. **12**(3): p. e0173486.
65. Singh, S.P., et al., *Selectivity in the Use of Gi/o Proteins Is Determined by the DRF Motif in CXCR6 and Is Cell-Type Specific.* Mol Pharmacol, 2015. **88**(5): p. 894-910.
66. Yu, X., et al., *CXCL16 induces angiogenesis in autocrine signaling pathway involving hypoxia-inducible factor 1alpha in human umbilical vein endothelial cells.* Oncol Rep, 2016. **35**(3): p. 1557-65.
67. Zhuge, X., et al., *CXCL16 is a novel angiogenic factor for human umbilical vein endothelial cells.* Biochem Biophys Res Commun, 2005. **331**(4): p. 1295-300.
68. Wang, Y.H., et al., *Vascular endothelial cells facilitated HCC invasion and metastasis through the Akt and NF-kappaB pathways induced by paracrine cytokines.* J Exp Clin Cancer Res, 2013. **32**(1): p. 51.
69. Han, X.H., et al., *Regulation of the follistatin gene by RSPO-LGR4 signaling via activation of the WNT/beta-catenin pathway in skeletal myogenesis.* Mol Cell Biol, 2014. **34**(4): p. 752-64.
70. Wicik, Z., et al., *The transcriptomic signature of myostatin inhibitory influence on the differentiation of mouse C2C12 myoblasts.* Pol J Vet Sci, 2011. **14**(4): p. 643-52.
71. Flamini, V., et al., *The Satellite Cell Niche Regulates the Balance between Myoblast Differentiation and Self-Renewal via p53.* Stem Cell Reports, 2018. **10**(3): p. 970-983.
72. Zhang, R., et al., *Chemerin induces insulin resistance in rat cardiomyocytes in part through the ERK1/2 signaling pathway.* Pharmacology, 2014. **94**(5-6): p. 259-64.
73. D'Alessandris, C., et al., *C-reactive protein induces phosphorylation of insulin receptor substrate-1 on Ser307 and Ser 612 in L6 myocytes, thereby impairing the insulin signalling pathway that promotes glucose transport.* Diabetologia, 2007. **50**(4): p. 840-9.
74. Coll, T., et al., *Palmitate-mediated downregulation of peroxisome proliferator-activated receptor-gamma coactivator 1alpha in skeletal muscle cells involves MEK1/2 and nuclear factor-kappaB activation.* Diabetes, 2006. **55**(10): p. 2779-87.
75. Klip, A., et al., *Signal transduction meets vesicle traffic: the software and hardware of GLUT4 translocation.* Am J Physiol Cell Physiol, 2014. **306**(10): p. C879-86.
76. Wang, X.Q., et al., *Trophoblast-derived CXCL16 induces M2 macrophage polarization that in turn inactivates NK cells at the maternal-fetal interface.* Cell Mol Immunol, 2018.
77. Cho, S.W., et al., *CXCL16 signaling mediated macrophage effects on tumor invasion of papillary thyroid carcinoma.* Endocr Relat Cancer, 2016. **23**(2): p. 113-24.
78. Kim, M.J., et al., *CXCL16 positively correlated with M2-macrophage infiltration, enhanced angiogenesis, and poor prognosis in thyroid cancer.* Sci Rep, 2019. **9**(1): p. 13288.
79. Krolopp, J.E., S.M. Thornton, and M.J. Abbott, *IL-15 Activates the Jak3/STAT3 Signaling Pathway to Mediate Glucose Uptake in Skeletal Muscle Cells.* Front Physiol, 2016. **7**: p. 626.
80. Ye, J., *Beneficial metabolic activities of inflammatory cytokine interleukin 15 in obesity and type 2 diabetes.* Front Med, 2015. **9**(2): p. 139-45.

81. Akieda-Asai, S., et al., *Interleukin-15 derived from Guanylin-GC-C-expressing macrophages inhibits fatty acid synthase in adipocytes.* Peptides, 2018. **99**: p. 14-19.
82. Lacraz, G., et al., *Deficiency of Interleukin-15 Confers Resistance to Obesity by Diminishing Inflammation and Enhancing the Thermogenic Function of Adipose Tissues.* PLoS One, 2016. **11**(9): p. e0162995.
83. Wu, H. and C.M. Ballantyne, *Skeletal muscle inflammation and insulin resistance in obesity.* J Clin Invest, 2017. **127**(1): p. 43-54.
84. Han, M.S., et al., *Regulation of adipose tissue inflammation by interleukin 6.* Proc Natl Acad Sci U S A, 2020. **117**(6): p. 2751-2760.
85. Stegmann, K.A., et al., *CXCR6 marks a novel subset of T-bet(lo)Eomes(hi) natural killer cells residing in human liver.* Sci Rep, 2016. **6**: p. 26157.
86. Thomas, S.Y., et al., *CD1d-restricted NKT cells express a chemokine receptor profile indicative of Th1-type inflammatory homing cells.* J Immunol, 2003. **171**(5): p. 2571-80.
87. Geissmann, F., et al., *Intravascular immune surveillance by CXCR6+ NKT cells patrolling liver sinusoids.* PLoS Biol, 2005. **3**(4): p. e113.
88. Shimaoka, T., et al., *Cutting edge: SR-PSOX/CXC chemokine ligand 16 mediates bacterial phagocytosis by APCs through its chemokine domain.* J Immunol, 2003. **171**(4): p. 1647-51.
89. Jiang, X., et al., *Cutting edge: critical role of CXCL16/CXCR6 in NKT cell trafficking in allograft tolerance.* J Immunol, 2005. **175**(4): p. 2051-5.
90. Bahr, I., et al., *Diet-Induced Obesity Is Associated with an Impaired NK Cell Function and an Increased Colon Cancer Incidence.* J Nutr Metab, 2017. **2017**: p. 4297025.
91. Spector, A.A., K. John, and J.E. Fletcher, *Binding of long-chain fatty acids to bovine serum albumin.* J Lipid Res, 1969. **10**(1): p. 56-67.
92. Cazzolli, R., et al., *A Role for Protein Phosphatase 2A–Like Activity, but Not Atypical Protein Kinase Cζ, in the Inhibition of Protein Kinase B/Akt and Glycogen Synthesis by Palmitate.* Diabetes, 2001. **50**(10): p. 2210-2218.